Acidity versus metal-induced Lewis acidity in zeolites for Friedel–Crafts acylation

Claire Bernardon, Manel Ben Osman, Guillaume Laugel, Benoît Louis, Patrick Pale

Full paper/Mémoire

Acidity versus metal-induced Lewis acidity in zeolites for Friedel–Crafts acylation

Claire Bernardon [a], Manel Ben Osman [a, *], Guillaume Laugel [b], Benoît Louis [a],
Patrick Pale [a]

[a] Laboratoire de Synthèse et Réactivité Organiques et Catalyse, Institut de Chimie, UMR 7177, 4, rue Blaise-Pascal,
67000 Strasbourg, France
[b] Sorbonne Universités, UPMC Univ Paris 06, UMR 7197, Laboratoire de Réactivité de Surface, 3, rue Galilée,
94200 Ivry-sur-Seine, France

A B S T R A C T

Acid catalysts including Ni, Ag and Fe-loaded zeolites of different structures were prepared either via cationic exchange or impregnation techniques from pristine H-zeolites (BEA, and MFI). Their catalytic activity was evaluated in the liquid-phase Friedel–Crafts acylation of anisole with propanoic acid. It turned out that, whatever the doping procedure was, the zeolite loaded with transition metals led to considerable decrease in propanoic acid conversion, regardless of the nature or the metal content. However, the extent of this detrimental effect followed the order: $Ag^+ > Ni^{2+} > Fe^{3+}$.
Pristine acidic zeolites were not only found to be the most active, but also to be the most selective toward *ortho*- and *para*-acylation products. H-ZSM-5 zeolites yielded the highest intrinsic activity, with TOF values of 0.09 h^{-1}. The catalyst activity proved to be essentially attributed to the density and accessibility of Brønsted acid sites, playing a key role in the activation of the reactants. Brønsted sites are proposed to be the most likely catalytic species for performing this Friedel–Crafts acylation.

© 2016 Académie des sciences. Published by Elsevier Masson SAS. This is an open access article under the CC BY-NC-ND license (http://creativecommons.org/licenses/by-nc-nd/4.0/).

R É S U M É

Des cations métalliques (Ni, Ag et Fe) ont été incorporés au sein de zéolithes BEA et ZSM-5 par des techniques d'échange cationique et d'imprégnation afin d'obtenir de nouveaux catalyseurs acides solides. Ces matériaux ont ensuite été testés dans une réaction d'acylation de Friedel–Crafts entre l'anisole et l'acide propanoïque en phase liquide. Il s'est avéré que l'ajout de métaux de transition au sein de la structure zéolithique entraîne une diminution considérable de la conversion, indépendamment de la nature ou de la quantité de métal introduite. Dans des conditions catalytiques similaires, les zéolithes parentes présentent une meilleure activité intrinsèque (TOF), en particulier H-ZSM-5, avec une production plus élevée de produits d'acylation (ortho- et para-), surpassant ainsi les performances catalytiques des zéolithes dopées par des métaux. L'accessibilité et la densité de sites acides de Brønsted se sont avérées déterminantes pour ce type de réaction.

© 2016 Académie des sciences. Published by Elsevier Masson SAS. This is an open access article under the CC BY-NC-ND license (http://creativecommons.org/licenses/by-nc-nd/4.0/).

* Corresponding author.
E-mail address: benosman@unistra.fr (M. Ben Osman).

1. Introduction

Friedel–Crafts reactions are among the most important C–C bond-forming transformations in organic chemistry, which have led to a wide range of applications. Among them, Friedel–Crafts acylation provides one of the most simple and powerful industrial routes to prepare aromatic ketones in high yields [1]. The so-formed aromatic compounds constitute valuable building blocks for fine chemistry, pharmaceutical, cosmetic and agrochemical industries, as well as for total synthesis of natural products [2,3].

The classical Friedel–Crafts acylation relies on homogeneous conditions in the presence of various Brønsted or Lewis acids. For the former, sulfuric acid, hydrofluoric acid or superacids are commonly used whilst for the later salts such as $ZnCl_2$, $AlCl_3$, $FeCl_3$, $SnCl_4$, and $TiCl_4$ have been used, often in super-stoichiometric amounts. More recently, rare-earth metal Lewis acids have been developed as efficient and true catalysts [4]. However, these reactions suffer from major drawbacks and disadvantages, due to the implication of strong acids and the requirement of stoichiometric or over-stoichiometric amounts of Lewis or Brønsted acids, with all the difficulties to recover and isolate the products from them, as well as the generation of large amounts of salty and acidic wastes.

On one hand, one way to minimize some of these problems is to perform Friedel–Crafts acylation directly with carboxylic acids as acylating agents, instead of their anhydrides or acyl chlorides, suppressing one step and the waste associated with it. On the other hand, a wide variety of heterogeneous acids have been explored as promoters in order to overcome those aforementioned environmental issues. Zeolites [5–7], clays [5], heteropolyacids [8,9], nafion [10], P_2O_5/SiO_2 [11] and solid "superacids", i.e. sulfate-supported metal oxides [12] and tungsto- or molybdophosphoric acids supported on [Zr, Ti, Sn] oxides [13], have been extensively studied in the general context of Friedel–Crafts reactions. Less extensive investigations have been performed for Friedel–Crafts acylations based on carboxylic acids as acylating agents. Here also, rare-earth metal salts proved to be efficient and true catalysts [14]. Interestingly, some acidic and modified zeolites have also been investigated in few cases [15,16]. Nevertheless, the combination of Lewis acid metal cations and zeolites has only been scarcely investigated in this context [17].

In the present contribution, we thus present preliminary results about the role of zeolites having different pore topologies, loaded with different metal cations at various loadings as catalysts for the Friedel–Crafts acylation of anisole with propanoic acid. The influence of the dealumination process was also briefly investigated. Furthermore, the performances of these zeolite catalysts have been compared with other solid acids, a heteropolyacid and two sulfated metal oxides (SnO_2, and ZrO_2).

2. Experimental

2.1. Pristine solid acid catalysts

Commercial zeolites, H-ZSM-5 (Zeolyst CBV5524 and CBV2314), H-BEA (Petrobras or Zeochem PB), H-USY (Zeolyst CBV500) and one home-made H-ZSM-5 [18], were activated under air atmosphere at 823 K for 12 h before use. Commercial $H_4SiW_{12}O_{40}$ heteropolyacid (Aldrich) and two sulphated oxides (SnO_2 and ZrO_2/SO_4^{2-}) were used as received.

2.2. Post-modifications of parent zeolites

2.2.1. Procedures for extra-framework aluminium (EFAl) exaltation and removal

In order to create extra-framework aluminium (EFAl) species, H-ZSM-5 and H-BEA were treated under *mild* steaming conditions: hydrothermal treatment was performed under nitrogen flow at 823 K for 24 h with water pre-heated at 323 K. This procedure is known to remove aluminium atoms from the framework [19]. To fully remove these EFAl species from the channels, a second treatment of these zeolites was performed by using Na_2H_2EDTA solution (EDTA = ethylenediaminetetraacetate) as described by T. Xu et al. [20].

2.2.2. Metal-loaded zeolites

Transition metals namely nickel, silver and iron, were introduced into pristine ZSM-5 and BEA zeolites (defined as parent) according to different procedures. Classical ion exchange in an aqueous phase and impregnation techniques were applied. These metal doping strategies are summarized hereunder:

Fe-loaded zeolites: iron was introduced into H-BEA$_{parent-2}$ zeolites by an incipient wetness impregnation technique using $Fe(NO_3)_3 \cdot 9H_2O$ solution at two different metal loadings: 0.25 and 10 wt%.

Ni-loaded zeolites: a dry impregnation procedure was performed on H-ZSM-5$_{parent-1}$ and H-BEA$_{parent-1}$ with nickel carboxylate as a precursor in toluene as described elsewhere [18]. The procedure was carried out in a rotary evaporator for 30 min at ambient temperature. The catalyst was dried for 1 h under vacuum at 393 K and then calcined in air at 873 K for 3 h.

Ag-loaded zeolites: silver was loaded in the ZSM-5$_{parent-2}$ zeolite as follows: the H-zeolite (2 g) was exchanged with a 0.1 M aqueous AgNO$_3$ solution (50 mL). The resulting white suspension was vigorously stirred overnight at 353 K in the absence of light. After the first cationic exchange, the solution was cooled, filtered through a nylon membrane (0.2 μm), washed with distilled water and dried in an oven for 24 h at 383 K. The resulting white powder was then submitted to a second ion exchange by following the aforementioned procedure. After drying for 24 h at 383 K, the solid was finally calcined at 823 K for 12 h under air to hinder silver reduction.

The as-obtained catalyst samples were referred to x%M-ZSM-5 and y%M-BEA zeolites (M corresponds to the metal introduced and x and y% to the amount initially used).

2.3. Characterisation of the catalysts

Although detailed characterisation of the zeolites was not the aim of the present study, the quantity of metal (wt %) and Si/Al ratios (SAR) were determined by XRF analyses. Specific surface areas were determined by N_2

adsorption–desorption isotherms following the BET method. The morphology of the particles was provided by Scanning Electron Microscopy (micrographs were acquired on a JEOL FEG 6700F microscope working at a 9 kV accelerating voltage) and the Brønsted acid site quantification was performed by H/D isotope exchange [21]. All data are summarized in Table 1.

Besides, XPS measurements of metal-promoted catalysts (1% Ni-ZSM-5$_{parent-1}$, 4% Ni-ZSM-5$_{parent-1}$, 10% Fe-BEA$_{parent-2}$, and 5.3% Ag-ZSM-5$_{parent-2}$) were carried out to understand the bonding state of the different metals in the zeolite framework. The X-ray Photoelectron Spectroscopy (XPS) measurements were performed with a hemispherical analyzer (SES R4000, Gamma data Scienta, pass energy 100 eV). The un-monochromatized AlKα X-ray source (1486.6 eV, 11 kV, 17 mA) without a charge neutralizer was applied to generate core excitation. The system was calibrated according to ISO 15472:2001. The energy resolution of the system, measured as a full-width at half-maximum (FWHM) for the Ag 3d$_{5/2}$ excitation line, was 0.9 eV. The powder samples were pressed into indium foil and mounted on a dedicated holder and then UHV evacuated. During the measurements, the pressure in the analysis chamber was roughly 10^{-9} mbar. The area of the sample analysis was approximately 3 mm^2. All binding energy (BE) values were charge-corrected to the carbon C$_{1s}$ excitation set at 285.0 eV. The Shirley-type background subtraction was used to the spectra prior to the fitting procedure, where Voigt line shape, i.e. Gaussian/Lorentzian functional (70:30) was applied.

2.4. Friedel–Crafts acylation

The activity of the catalysts was evaluated in the reaction between anisole and propanoic acid (Fig. 1) according to the following protocol:

The solid acid (iso-mass conditions, 250 mg) was added to a mixture of anisole (10 mmol, Sigma–Aldrich) and propanoic acid (2.5 mmol, Sigma–Aldrich) in a closed reactor system. Upon sealing, the tube was heated at 423 K for 24 h. After this duration and cooling, the crude was filtered on a Nylon Millipore membrane (0.2 μm) with CDCl$_3$ as a filtration solvent and analysed by ^{1}H NMR and GC–MS.

The products were identified and characterised by ^{1}H NMR recorded on a Bruker Avance Spectrometer at 300 MHz. Chemical shifts are given in parts per million

(ppm) on the delta scale. The solvent peak was used as a reference value (for ^{1}H NMR: CDCl$_3$ = 7.26 ppm). GC–MS analyses were performed with a TSQ Quantum (Thermo scientific) MS detector, equipped with a HP5-MS column (30m × 0.25 mm × 0.1 μm).

3. Results and discussion

3.1. The reaction between anisole and propanoic acid

Under the reaction conditions, a mixture of compounds was produced (Fig. 1). The expected *ortho* and *para* acylated compounds **3** were the main reaction products. Besides, the acylated phenols **4** were also isolated as well as the phenyl propanoate **5**.

The latter was probably formed by anisole demethylation followed by acylation. Compounds **4** could thus be produced either by Fries rearrangement of this ester or by demethylation of compounds **3**.

Concerning the distribution of the products, the main products formed over all samples are **3**, *ortho* and *para*, regardless of the zeolites used. *Ortho-* and *para*-acylated products were produced in a 2:1 ratio over most of the solids, revealing that this reaction is not governed by shape-selectivity. We have therefore decided to focus the rest of this work on acylated products **3** selectivity. It is wise to mention that the impact of the metal content on the selectivity could not be easily discussed because of large differences in the conversion levels.

The activity of the catalysts was measured after 24 h of reaction and during this period no significant deactivation phenomenon seemed to occur. Also, it is worth noting that the leaching process was evaluated to assess if metallic species were removed from the catalyst into the solution. The reaction was stopped after 24 h and the catalyst was removed by filtration. The recovered zeolite was calcined under air and then reused under the same conditions and the same PA conversion level could be achieved. Hence, leaching of metallic active species was discarded, thus indicating a true heterogeneous catalysis of metal-loaded zeolite catalysts.

3.2. Screening of solid acids

Classical ion exchange methods allowed introducing nickel, silver and iron into ZSM-5 and BEA zeolites (Table 1).

Table 1

M^{n+} zeolite catalysts prepared by ion exchange and impregnation methods: Si/Al ratio, SSA values, number of Brønsted acid sites and metal amount (wt%).

| Catalysts	Metal amount (wt% XRF)	Si/Al ratio	SSA (m^2/g)	Acidity (mmol H$^+$/g catalyst)
H-ZSM-5$_{parent-1}$	–	12.5	392	1.58
1% Ni-ZSM-5$_{parent-1}$	1	–	332	1.43
4% Ni-ZSM-5$_{parent-1}$	3.65	17.4	319	1.24
H-ZSM-5$_{parent-2}$	–	11.5	425	1.48
2.6% Ag-ZSM-5$_{parent-2}$	0.01	15.3	–	1.60
5.3% Ag-ZSM-5$_{parent-2}$	0.03	15.5	–	1.16
H-BEA$_{parent-1}$	–	14.9	–	2.35
1%Ni-BEA$_{parent-1}$	1	16.2	–	1.33
H-BEA$_{parent-2}$	–	13.8	485	1.63
0.25% Fe-BEA$_{parent-2}$	7.2	–	–	1.40
10% Fe-BEA$_{parent-2}$	12.4	14.8	379	0.85
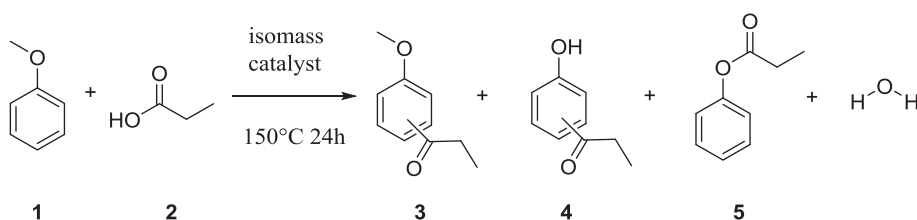
Fig. 1. Friedel−Crafts acylation of anisole with propanoic acid.

In these metal-loaded zeolites, SAR ratios slightly increased compared to the parent zeolites, indicating that metal ions probably exchanged some of EFAl species naturally present. However, specific surface areas diminished after the addition of metal, whatever the type of the zeolite structure (MFI or BEA), suggesting the presence of metal species inside the porous network. Likewise, the concentration of Brønsted acid sites decreased while raising the metal amount for doping the zeolites, thus confirming an exchange between metallic species and protons. XRF analysis provided the amount of metal loaded within the zeolites (Table 1). The collected values revealed that the metal introduction was not proportional to the quantity initially used. However, the metal introduction proved to be sensitive to the metal nature as well as to the introduction methodology [17].

It is also noteworthy that the Brønsted acid site consumption, after the metal loading procedure, was more pronounced with zeolites possessing the highest Brønsted acid site density (BEA zeolite$_{parent-1}$ with 2.35 mmol/g). This suggests that the acid site density and their proximity may have an influence on the metal introduction into the zeolite pores.

The EDTA-treated ZSM-5 zeolite led to achieve a higher SAR value, i.e. roughly 20 with respect to 12, before the complexation treatment. Indeed, extra-framework aluminium species have been removed from the zeolites. Regarding the steamed samples, we did not observe a significant variation in bulk SAR values when compared to pristine zeolites (indeed, XRF analysis is unable to distinguish framework and extra-framework species).

To check the possible structure changes or collapse of the zeolite framework during the post-synthesis modifications, XRD analysis was performed. The related XRD patterns (not shown) confirmed the preservation of zeolite structures in promoted samples, in agreement with earlier reports [22,23]. The presence of metal oxides (possibly formed after the calcination step) could be discarded based on these XRD patterns. One may therefore expect that metal cations are well dispersed within the zeolite and probably present in a rather isolated form. It is important to point out that the strength of metal coordination, localization and distribution among all the catalysts may be different, all these features being directly related to the catalytic behaviour. The obtained catalysts were applied to the reaction described above (Fig. 1).

The solid acids have been evaluated under isomass conditions in the FC reaction between anisole and propanoic acid. According to Fig. 2, H-ZSM-5 and H-BEA zeolites exhibited the highest propanoic acid conversion among all solid acids. Sulfated metal oxides as well as amorphous silica-alumina were barely active in this reaction, thus indicating the importance of decent pore sizes as well as a need for strong acidity. While the highest conversion was achieved over H-ZSM-5, the highest selectivity in acylated products **3** was achieved over the H-BEA zeolite (70%). Hence, one may suggest that the catalytic reaction is occurring on the external surface for ZSM-5 zeolite, whilst
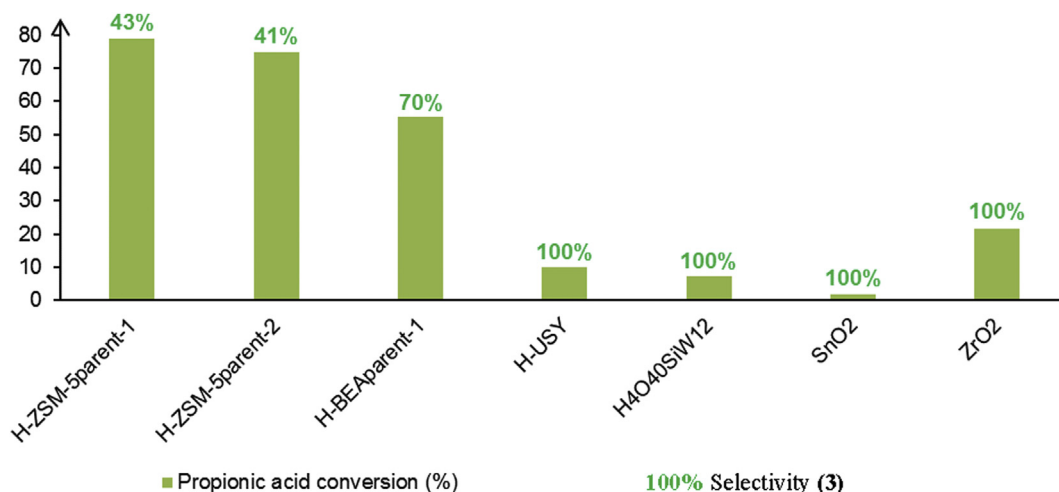

Fig. 2. Acylation products (**3**) selectivities and PA conversions achieved over solid acids in the reaction between anisole and propanoic acid.
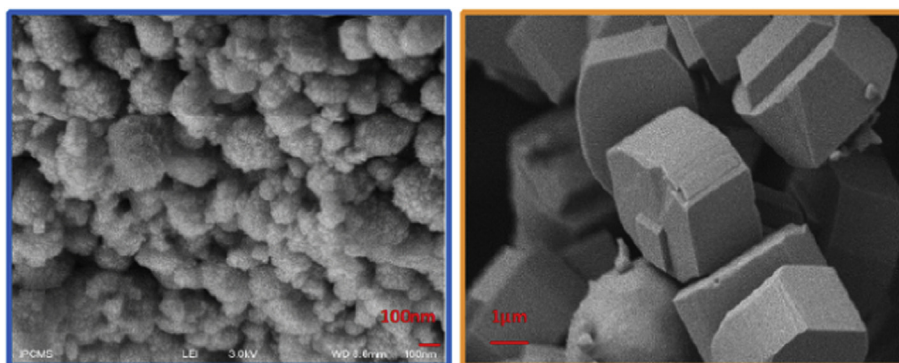
Fig. 3. SEM images of **BEA** (left) and **ZSM-5** (right) crystals.

it takes place within the pores of H-BEA catalyst. In contrast, FAU-type structure seems rather inefficient for this reaction in terms of PA conversion.

H-ZSM-5 and H-BEA zeolites are promising catalysts for this acylation reaction, according to former studies [24–27]. Their two peculiar pore topologies [28] seem beneficial for achieving a high PA conversion and were therefore selected as hosts for metallic sites. Fig. 3 presents the SEM micrographs of BEA and MFI (parent-1) catalysts. The BEA zeolite exhibits an arrangement of nanocrystals, whilst ZSM-5 crystals possess a coffin-shape with few micrometers in size (3–5 μm). The pore accessibility may also be a key parameter to reach a better catalytic performance [29].

The influence of the SAR parameter in the present acid catalysis has also been investigated (Table 1). The conversion of propanoic acid remained roughly the same, 75% and 79% with SAR values of 11.5 and 12.5 for H-ZSM-5$_{parent-2}$ and H-ZSM-5$_{parent-1}$, respectively. Based on H/D exchange technique (Table 1), H-BEA$_{parent-1}$ exhibits a 45% higher number of Brønsted sites with respect to H-BEA$_{parent-2}$ and yet the conversion reached higher values, i.e. 55% versus 25% (Table 2). This trend is usually observed since a higher Al-content (low SAR) means 'a priori' more Brønsted sites but also more Lewis sites.

The BEA zeolite exhibits the highest density of Brønsted sites but did not lead to the highest PA conversion (Fig. 2);

obviously other factors must contribute to enhance the activity. We tempt to state that acidity type and distribution are determinant factors for this reaction, in line with former studies [7,30].

3.3. Influence of extra-framework aluminium content on the activity

EFAl introduction into zeolites has already been proved to enhance catalytic performances in several acid-catalysed reactions [31]. The raise in activity was either attributed to the creation of mesoporosity after steaming treatment [19] or to a polarisation effect of cationic extra-framework aluminium species present in the vicinity of Brønsted acid sites [32].

EFAl species are often reported to be active acid sites, even if their nature and how they affect the Brønsted acidity of zeolites is still a matter of debate. EFAl species can occupy cationic positions or be present as intra-zeolite oxide species. It has been postulated that the latter species may exist in different forms such as Al^{3+}, AlO^+, $Al(OH)_2^+$ and $AlOH^{2+}$ and also as monomeric $AlOOH$, $Al(OH)_3$ or even clusters [32]. Fig. 4 highlights the fact that dealuminated zeolites with steam improved PA conversion when compared to pristine zeolites, regardless of the zeolite type. PA conversion was slightly increased from 43% to 49% for BEA and from 62% to 69% for ZSM-5 samples

Table 2
Propanoic acid conversion and selectivity toward acylated products (*ortho*- and *para*) over Ag, Ni, and Fe loaded zeolites.

Catalysts	Si/Al[a]	PA Conversion %[b]	Selectivity 3 (*ortho* + *para*)%[b]	Yield 3 (*ortho* + *para*)%[b]	TOF (h^{-1})[c]
H-ZSM-5$_{parent-1}$	12.5	79	43	34	0.088
1% Ni-ZSM-5$_{parent-1}$	16.2	23	55	13	0.037
4% Ni-ZSM-5$_{parent-1}$	17.4	23	55	12	0.042
H-ZSM-5$_{parent-2}$	11.5	75	41	31	0.086
2.6% Ag-ZSM-5$_{parent-2}$	15.3	3	100	3	0.008
5.3% Ag-ZSM-5$_{parent-2}$	15.5	4	100	4	0.014
H-BEA$_{parent-1}$	14.9	55	70	39	0.069
1%Ni-BEA$_{parent-1}$	16.2	26	73	19	0.063
H-BEA$_{parent-2}$	13.8	25	76	19	0.048
0.25% Fe-BEA$_{parent-2}$	–	20	77	15	0.045
10% Fe-BEA$_{parent-2}$	14.8	13	100	13	0.063

[a] SAR determined by XRF measurements.
[b] Estimated from ^1H NMR.
[c] Calculations based on Brønsted acid site density (mmol **3**/mmol H$^+$/h).
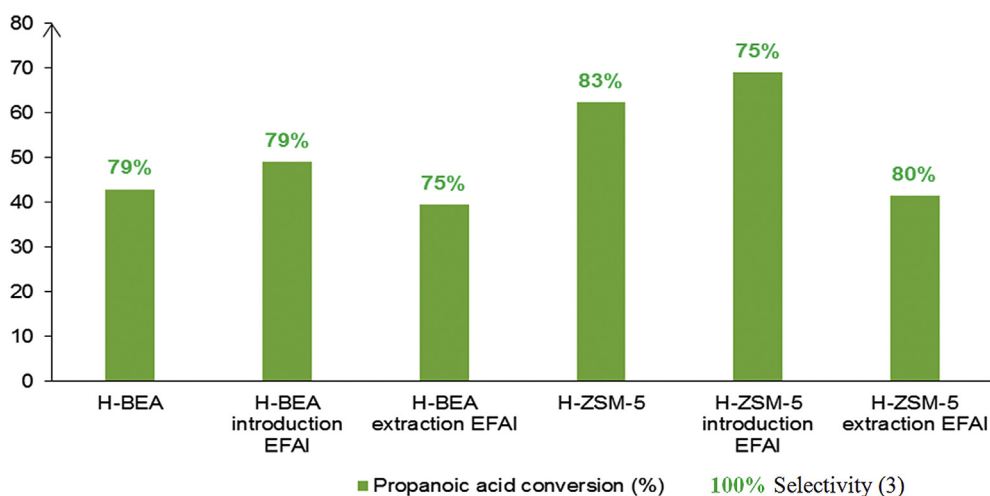
Fig. 4. Sequential extra-framework aluminium introduction and removal in BEA and ZSM-5 zeolites and their reactivity in the acylation reaction.

without a significant loss in selectivity toward acylated products **3**.

Furthermore, when EFAl species were removed using EDTA as a complexing agent, PA conversions declined, notably in the case of the ZSM-5 zeolite with smaller pore size, even if the selectivity to acylation products **3** remained nearly constant. These results showed that Lewis acidity associated with EFAl species appears beneficial for the catalytic process for both commercial catalysts.

3.4. Catalytic activity of metal-exchanged zeolites

Hence, various transition metals, acting as Lewis acid sites were exchanged within the zeolites to further try to enhance the activity of the parent catalysts. All metal-exchanged zeolites were evaluated as catalysts for the acylation of anisole with PA and subsequently compared to their pristine H-zeolite form.

The catalytic performances of these metal-promoted zeolites at different loadings are listed in Table 2. These data clearly assess a decrease in propanoic acid conversion over all metal-doped catalysts compared with pristine zeolites. However, these modifications induced by the metal presence are dependent on the nature and/or the metal loading.

3.4.1. Ag- and Ni-ZSM-5 catalysts

The XRF chemical analysis revealed that the Ag loading reached 0.24 mmol/g after two cationic exchange steps. Therefore, Ag ions have substituted approximatively one sixth of the Brønsted acid site population in H-ZSM-5$_{parent-2}$ (1.48 mmol/g). The incorporation of silver by an ionic exchange method into the H-ZSM-5$_{parent-2}$ zeolite at a low level of exchange (below 0.1%) might indicate the formation of isolated silver essentially located as a compensation cation in the zeolite framework. However, a drastic decrease in the PA conversion, compared with pristine H-ZSM-5 zeolite, was noticed from 75% to 3–4% after doping with silver. Despite the low silver loading in the zeolite (0.01 wt% after one cationic exchange and 0.03 wt% after the second exchange), it appears that a strong inhibition

occurred during the acid-catalysed reaction. Such a detrimental effect in catalysis is most probably due to the presence of silver as nanoparticles at the zeolite external surface which may hinder the pore accessibility. The presence of Ag nanoparticles in Ag-FAU was already evidenced by our team using TEM analysis (data not shown). Indeed, for the 5.3% Ag-ZSM-5$_{parent-2}$ sample, a symmetric and narrow Ag 3d$_{5/2}$ peak could be detected by XPS centred at 368.6 eV. This value suggests that silver is exclusively present in the zeolite as metallic Ag.

Regarding nickel-based catalysts, an important decrease in PA conversion was observed, from 79% to 23% with 1% Ni-ZSM-5 and 4% Ni-ZSM-5 zeolites. The latter zeolites have been thoroughly characterised using synchrotron techniques [18,33] and a mixture of cationic Ni^{2+} compensation cation and NiO species formed within the zeolite channels was ascertained. This is perfectly in line with XPS data. The Ni 2p$_{3/2}$ XPS spectra for 1% Ni-ZSM-5$_{parent-1}$ and 4% Ni-ZSM-5$_{parent-1}$ are presented in Fig. 5. For the sample with 1% Ni loading, this peak could be deconvoluted into three components, one centred at 854.6 eV and the two others at 857.9 eV and 860.4 eV, respectively (Fig. 5a). Taking into account that the binding energy (BE) for unsupported NiO is 853.7 eV, the peak at 854.6 eV may be assigned to Ni^{2+} in octahedral sites of the supported NiO structure, and the peak at 857.9 eV may be associated with Ni^{2+} in tetrahedral positions of a spinel-like structure of Ni–Al oxide [34]. This tetrahedral environment might be the result of the solid-state diffusion of Ni^{2+} into the pores during the calcination process [35]. The last peak centred at 860.4 eV may be attributed to Ni^{2+} located inside the zeolite channel as compensation cations.

In the case of the Ni 2p$_{3/2}$ XPS spectrum of 4% Ni-ZSM-5$_{parent-1}$ only two contributions (855.6 eV and 857.8 eV) could be detected, being assigned to the Ni cation after the deconvolution procedure (Fig. 5b). Based on the discussion regarding the Ni 2p$_{3/2}$ spectrum of 1% Ni-ZSM-5$_{parent-1}$, the first peak centred at 855.6 eV corresponds to Ni^{2+} in NiO species. The second peak agrees with a binding energy in line with Ni–Al oxide structure. However, the first peak
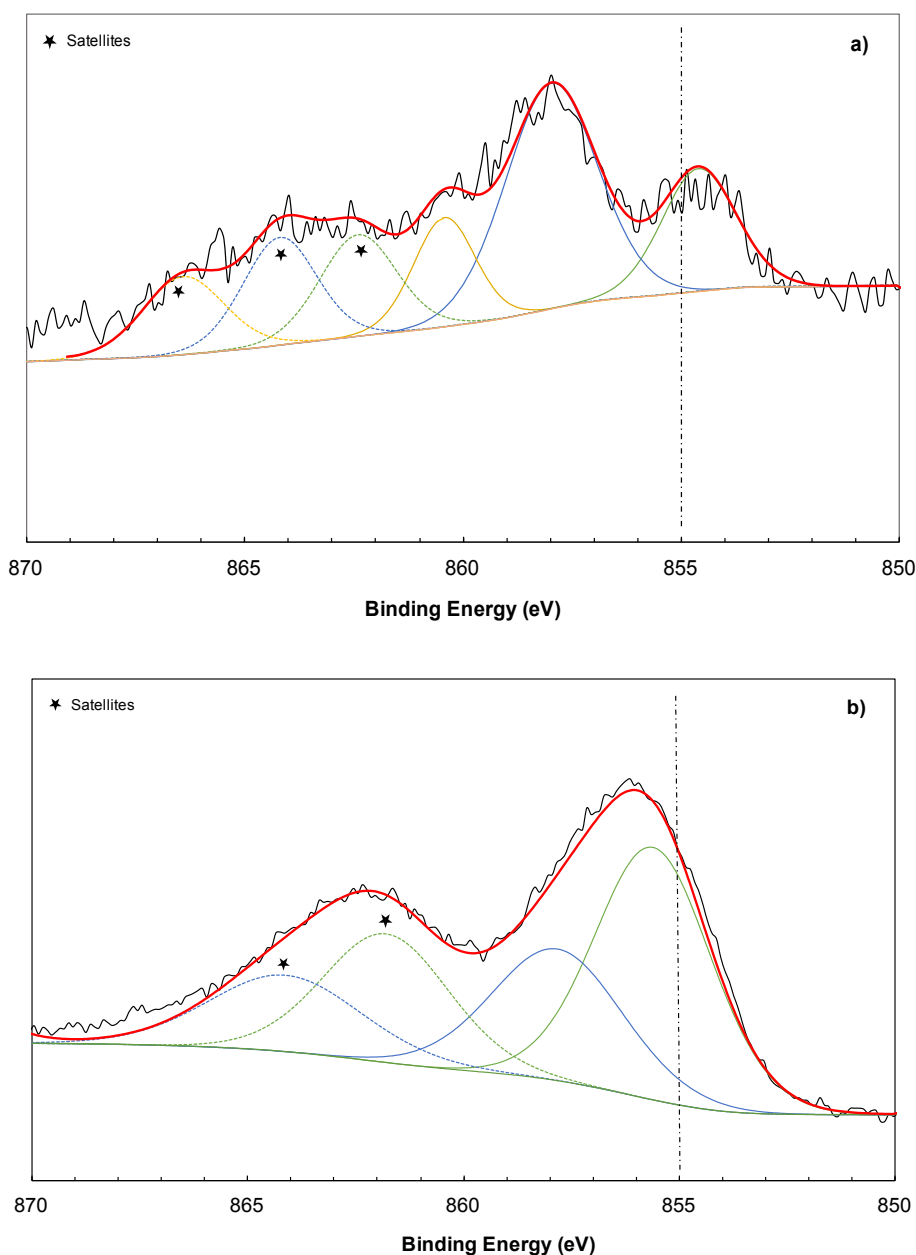
Fig. 5. XPS spectrum of Ni 2p$_{3/2}$ for 1% Ni-ZSM-5$_{parent-1}$ (a) and 4% Ni-ZSM-5$_{parent-1}$ (b).

shifts to higher BE values from 854.6 to 855.6 eV at higher nickel loading. This new BE value suggests that the environment of Ni^{2+} ions in Ni (4% wt) is different from the one in Ni (1% wt) and may be assigned to Ni^{2+} in Ni(OH)$_2$ as proposed by Grosvenor et al. [36]. Furthermore, it is noteworthy that 4% Ni-ZSM-5$_{parent-1}$ exhibits a more obvious first peak than in the zeolite with lower Ni loading, thus indicating a larger amount of Ni^{2+} on the surface than in the 1% Ni-ZSM-5$_{parent-1}$ sample. This increase in the intensity of the low energy peak can be the consequence of the decreased diffusion of Ni^{2+} in the zeolite pores.

The detrimental effect of nickel species on the Friedel−Crafts acid catalysis is less pronounced than for silver

species. In terms of selectivity, a loading with more nickel species did not alter the formation of acylated products **3**. Whatever the nature or the amount of the metal used (Ni, Ag), pristine H-ZSM-5 zeolites proved to be the most active and selective catalysts with yields in the range of 30−40% toward the desired products (Table 2).

3.4.2. Ni- and Fe-BEA zeolites

The acylation of anisole was also performed over nickel and iron-doped BEA zeolites. Likewise to Ni-ZSM-5 zeolites, 1 wt% Ni-BEA$_{parent-1}$ led to a large decrease in PA conversion from 55% to 26% over BEA$_{parent-1}$ (Table 2). Surprisingly, the same selectivity in acylation products was

reached and TOF values were equal (this parameter is formulated as the quantity of acylated products formed (**3**) per mole of acid sites in one hour); this behaviour is different from the one observed for Ni-ZSM-5 zeolites. The loading of 1 wt% of Ni by impregnation on BEA zeolites may favour the formation of small nickel particles in contrast to its distribution as compensation cation. As a result, the lower PA conversion reached over Ni-BEA zeolites could be ascribed to faster coke formation on nickel or NiO particles. It is also surprising that for ZSM-5$_{parent-1}$ and BEA$_{parent-1}$ zeolites promoted with the same Ni content (1 wt%) exhibited similar PA conversion (23% and 26%, respectively). However, at a similar Ni loading (1 wt%), the decrease in the conversion was more pronounced for the ZSM-5 zeolite than that for the BEA zeolite compared to their related pristine materials. This behaviour may be attributed to different natures of Ni species or different distributions depending on the zeolite structure as well as the pore system in BEA zeolites. A higher anisole and carboxylic acid accessibility should be allowed in the BEA zeolite framework. Despite the decrease in PA conversions upon Ni introduction into BEA zeolites, no significant variation in *ortho*- and *para*-acylation products (**3**) could be observed.

0.25 wt% and 10 wt% Fe-BEA$_{parent-2}$ zeolites also exhibited lower PA conversions (20% and 13%, respectively) when the amount of iron was enhanced with respect to the parent BEA zeolite. The significant decrease in SSA values observed between H-BEA$_{parent-2}$ (485 m^2/g) and 10 wt% Fe-BEA$_{parent-2}$ zeolites (379 m^2/g) in Table 1 suggests the presence of Fe oxides probably as disordered crystallites due to the absence of characteristic peaks in the XRD pattern [37]. Concerning the sample 10% Fe-BEA$_{parent-2}$, the Fe 2p$_{3/2}$ XPS spectra could be described by two components, one centered at 710.6 eV and the second at 711.8 eV. According to Gurgul et al. [38], all BE of the Fe$_{3/2}$ lines are higher than 710.5 eV, which strongly suggests that iron is present as Fe^{3+} species in two different environments. Furthermore, the same authors excluded by Mössbauer spectroscopy the presence of non-framework iron (Fe$_3$O$_4$ and Fe$_2$O$_3$).

This comparison showed that the catalyst without any iron introduction (BEA zeolite$_{parent-2}$) is still more active than Fe-doped BEA zeolites, generating a slightly higher yield in *ortho*- and *para*-acylation products (**3**) (i.e. 19% for H-BEA$_{parent-2}$ versus 15% and 13% for Fe-BEA zeolite$_{parent-2}$). It is important to point out that the negative effect of metal introduction is less pronounced for Fe-doped zeolites. Indeed, TOF values are comparable with pristine H-zeolites, indicating that the intrinsic catalyst performance is equal. In addition to their negative role related to the substitution of protons, silver and nickel species also appear detrimental in terms of TOF, suggesting an inhibiting effect of metallic species. In contrast, iron species appear rather inactive for this FC acid-catalysed reaction. The same tendencies were observed by Cruz-Cabeza et al. [23] who highlighted a non-beneficial effect of Ni in BEA zeolites on acylation reactions.

At this point of the study, it is worth mentioning that more or less drastic decreases in activity and selectivity were obtained over metal-loaded zeolites. This can be assigned to the modification of the acidity in the host

zeolites. It is therefore questionable whether such hampered catalytic behaviour is rather related to the creation of metallic Lewis acid sites or to the decrease of Brønsted acid sites or to their limited accessibility.

3.5. Rationalization of the active acid site nature

The respective role of Brønsted acid sites and metal species in the catalytic behaviour of zeolites is still controversial to date. Consequently, we were interested in the identification of the nature of the acid sites really acting as active species to get insight into the understanding of how metal-modified zeolites behave as catalysts. Generally, it is claimed that the reactants could be activated on Brønsted and/or Lewis acid sites present in metal-loaded zeolites [17]. Two activation paths may therefore be expected: **i**) either direct involvement of the metal species and/or **ii**) direct involvement of the remaining Brønsted acid sites as active sites. According to the data presented in Table 2, PA conversion was not directly proportional to the density of Brønsted acid sites, this feature might demonstrate that it is not possible to consider the sole Brønsted acid sites for performing the FC reaction.

The density and nature of the two kinds of acid sites were carefully considered to tempt any rationalization of the catalyst behaviour. It has already been assessed that the accessibility and the relative content in Lewis and Brønsted acid sites strongly depend on several factors, namely the topology of the zeolite, the SAR, and the water formation during the reaction under batch conditions at 423 K which may complicate the discrimination between Lewis and Brønsted sites [17]. As reported elsewhere [22], the catalytic performances might be modulated by a possible involvement of species generated after calcination such as additional dispersed metal oxide species. Hence, the influence of these species on the catalysis cannot be completely ruled out. The investigation of the role of metallic species on catalyst's activity can be complicated by the difficulty to identify their structure.

Regarding the aforementioned observations, metal-modified zeolites were less effective in the Friedel–Crafts reaction than their parent counterparts, regardless of the nature of the metal species. Bare protonic zeolites exhibited higher activity than Lewis acid metal-zeolites which highlight the detrimental role of metal species incorporated in the zeolites (even limited in the case of iron). Indeed, the PA conversion diminished according to the following order: H-zeolite > Fe > Ni > Ag. The influence of Ag on PA conversion was more significant compared with the other metals, due to higher Lewis acidity of Ag$^+$ exchanged over zeolites. In addition, even after incorporation at higher amounts into BEA zeolites ($\geq$7 wt%), the presence of iron led only to a moderate decrease in PA conversion with respect to H-BEA zeolites. It is important to point out that the classification is correlated to the strength of the Lewis acid sites created by exchanged metal cations. The higher the Lewis acidity (Ag$^+$ > Ni^{2+} > Fe^{3+}), the more severe decrease in activity could be observed.

In contrast to what is usually considered for other reactions [33,39,40], the relative enrichment of zeolites in Lewis acidity seems detrimental for PA conversion. The

reactivity of all zeolites was negatively impacted by the introduction of Lewis acidity induced by the metals. M^{n+} might stabilize too strongly the intermediate species than remaining H^+ and therefore rather act as a limiting actor toward reactivity. Moreover, there might be an adsorption competition between the reactants on Lewis and Brønsted acid sites, leading to slower acylation rates. The lower selectivity exhibited by promoted zeolites can be attributed to the presence of strong Lewis acid sites that are able to catalyse consecutive reactions, leading to the formation of undesired products. This confirms that metal species are not necessary to yield acylated products **3**.

The content and accessibility of metals (present as oxides or metal cations) play a role in the modification of acidic properties by modulating the density of Brønsted acid sites. The addition of metals may not only affect the strength of these acid sites but also diminish their concentration. Indeed, ion exchange and impregnation methods resulted in a decrease of Brønsted acidity while new Lewis acid sites were generated (Table 1). The TOF was calculated, assuming that all Brønsted groups can act as catalytically active sites, to reveal the intrinsic activity of the samples. For the Ni-ZSM-5$_{parent-1}$ samples, TOF values remained nearly identical for H-ZSM5$_{parent-1}$ (0.088 mmol **3**/mmol H^+/h). TOF diminished over 1 wt% Ni-ZSM5$_{parent-1}$ (0.037 mmol **3**/mmol H^+/h) and 4 wt% Ni-ZSM5$_{parent-1}$ (0.042 mmol **3**/mmol H^+/h). This may be associated with the presence of inactive metallic species formed at a loading of up to 1 wt%.

Surprisingly, two distinct relationships between TOF values and the density of Brønsted acid sites could be established for BEA and ZSM-5 zeolites (Fig. 6). Whilst the TOF only suffered minor modifications as a function of the density of Brønsted acid sites in BEA, the ZSM-5 zeolite exhibited a continuous TOF raise with increasing acidity. It indicates that the presence of metallic species in BEA channels neither hinder the reactant adsorption nor the product desorption. In contrast, the presence of metals in the ZSM-5 zeolite led to seriously diminish TOF values. In addition to substitute active protons for the reaction, metal species further prevent the smooth progress of the reaction. This might probably be due to a hindered accessibility in ZSM-5 medium-sized pores. The dependence of TOF values with Brønsted acidity on the ZSM-5 surface supports the higher probability for the FC reaction to proceed at the external surface (or at the pore-mouth entrance) as highlighted previously (based on data presented in Fig. 2).

However, a general tendency clearly shows that TOF values achieved over doped zeolites are globally lower than those of pristine zeolites, disclosing the incorporation of metal ions as a crucial parameter to reach a high activity in the Friedel—Crafts reaction. This consideration strongly supports that the active acid site is of Brønsted nature, as reported for a large palette of catalytic reactions [7,29,41,42].

One could consider that metal sites are competing with Brønsted sites as active sites involved in the catalytic process but the more relevant contribution is certainly attributed to Brønsted acid sites. Consistently, no acylation product was obtained when the Na-zeolites were employed as catalysts, reinforcing the direct involvement of Brønsted acid sites in the formation of acylation products. It has already been reported that the higher density of acid sites is a crucial parameter to enhance the activity in the acylation reaction [43]. The presence of numerous acyl carbocations, generated by a higher density of Brønsted acid sites, impacts the electrophilic substitution with the carboxylic acid to produce acylated products.

Many reactions catalysed by Brønsted acidity have been studied in the past. In the present study, the importance of this type of acid sites was checked again. A direct comparison between H-zeolites and Ag, Ni, and Fe was made and revealed the prominence of Brønsted acid over Lewis acid solids. Our experimental results emphasize that the
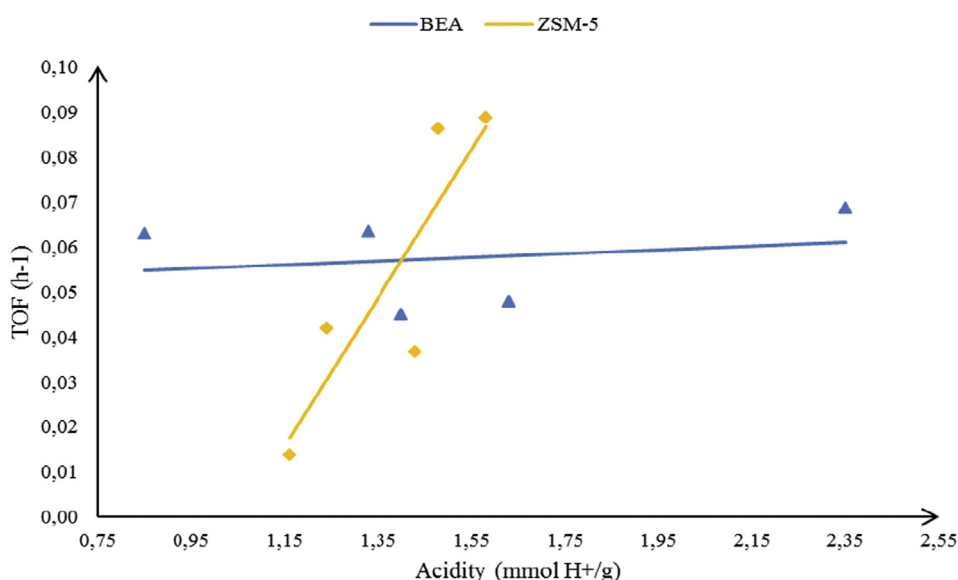

Fig. 6. TOF value dependence to the Brønsted acid site density (BEA and ZSM-5 zeolites).

Lewis acid sites created by the incorporation of metal into zeolites are not promising candidates for this reaction. The inhibiting effect of the introduction of metals is pointing toward an optimal role of the Brønsted acidity. The Friedel—Crafts reaction seems to be preferably promoted by a high amount of Brønsted acid sites, and thus favoured in pristine zeolites with respect to heterogeneous Lewis acid catalysts. H-zeolites are definitely the most efficient catalysts in terms of TOF for this acylation reaction in comparison to metal-doped zeolites (and sulfated metal oxides). In this context, H-ZSM-5 zeolites exhibited the highest TOF values (>0.08 mmol **3**/mmol H^+/h) among parent and doped BEA, confirming that the pore structure is also essential for this reaction.

Herein, we demonstrated the great potential of H-zeolites for this catalytic application, in which Brønsted acid sites appear to play the key role. Given that, the reactivity might be dependent on the speciation of metal introduced into different zeolite structures, the nature of metal species deserves further investigation via various techniques such as TEM, diffuse reflectance UV—vis, TPR, NMR and XPS.

4. Conclusion

Friedel—Crafts acylation of anisole with propanoic acid was investigated in the liquid-phase using H-ZSM-5 and H-BEA zeolites, as well as their corresponding Ag, Fe, and Ni doped counterparts. All metal-loaded zeolites prepared by ion exchange and impregnation techniques exhibited lower PA conversions compared to their parent zeolites, regardless of the nature or the metal content. This result could be explained by an increase of Lewis acid sites created upon by the loading procedure. Nevertheless, the extent of the activity drop varied from one metal to another following this order (Ag > Ni > Fe). Interestingly, metals acting as Lewis acid sites appeared to be detrimental for the PA conversion level, and for the selectivity in targeted ortho- and para-acylation products. The pristine ZSM-5 zeolite was found to be the most promising catalyst for the Friedel—Crafts acylation with the highest intrinsic activity (TOF) close to $0.09 \ h^{-1}$.

References

[1] G. Rothenberg, Catalysis: Concepts and Green Applications, Wiley, 2008.
[2] G.A. Olah, Friedel—Crafts and Related Reactions, Interscience, New York, 1963—1965.
[3] I. Houssini, M.A. Harrad, B. Boualy, A. Ouahrouch, M. Loughzail, M. Ait, A. Karim, Chem. Mater. Res. 6 (2014) 1—6.
[4] (a) N. Mine, Y. Fujiwara, H. Taniguchi, Chem. Lett. (1986) 357—360;
(b) A. Kawada, S. Mitamura, J-I. Matsuo, T. Tsuchiya, S. Kobayashi, Bull. Chem. Soc. Jpn. 73 (2000) 2325—2333.

[5] (a) D.E. Akporiaye, K. Daasvatn, J. Solberg, M. Stöcker, Stud. Surf. Sci. Catal. 78 (1993) 521—526;
(b) G. El Hiti, K. Smith, A.S. Hegazy, Curr. Org. Chem. 19 (2015) 585—598.
[6] S. Borghèse, P. Drouhin, V. Bénéteau, B. Louis, P. Pale, Green Chem. 15 (2013) 1496—1500.
[7] P.B. Venuto, Micropor. Mater. 2 (1994) 297—411.
[8] H. Firouzabadi, N. Iranpoor, F. Nowrouzi, Tetrahedron 60 (2004) 10843—10850.
[9] I.V. Kozhevnikov, Appl. Catal., A 256 (2003) 3—18.
[10] G. Sart ori, R. Maggi, Chem. Rev. 106 (2006) 1077—1104.
[11] A. Zarei, A.R. Hajipour, L. Khazdooz, Tetrahedron Lett. 49 (2008) 6715—6719.
[12] K. Arata, Green Chem. 11 (2009) 1719—1728.
[13] S.V. Ghodke, U.V. Chudasama, Int. J. Chem. Stud. 2 (2015) 27—34.
[14] (a) P.H. Tran, P.E. Hansen, H.T. Nguyen, T.N. Le, Tetrahedron Lett. 56 (2015) 612—618;
(b) M. Kawamura, D.-M. Cui, T. Hayashi, S. Shimada, Tetrahedron Lett. 44 (2003) 7715—7717;
(c) M. Kawamura, D.-M. Cui, S. Shimada, Tetrahedron 62 (2006) 9201—9209.
[15] S.G. Wagholikar, P.S. Niphadkar, S. Mayadevi, S. Sivasanker, Appl. Catal., A 317 (2007) 250—257.
[16] (a) Y. Ma, Q.L. Wang, B. Zuo, Appl. Catal., A 165 (1997) 199—206;
(b) C. De Castro, J. Primo, A. Corma, J. Mol. Catal. 134 (1998) 215—222;
(c) G. Bai, J. Han, H. Zhang, C. Liu, X. Lan, F. Tian, Z. Zhao, H. Jin, RSC Adv. 4 (2014) 27116—27121.
[17] C. Gauthier, B. Chiche, A. Finiels, P. Geneste, J. Mol. Catal. 50 (1989) 219—229.
[18] A.J. Maia, B. Louis, Y.L. Lam, M.M. Pereira, J. Catal. 269 (2010) 103—109.
[19] S. van Donk, A.H. Janssen, J.H. Bitter, K.P. de Jong, Catal. Rev. Sci. Eng. 45 (2003) 297.
[20] T. Xu, H. Song, W. Deng, Q. Zhang, Y. Wang, Chin. J. Catal. 34 (2013) 2047—2056.
[21] B. Louis, S. Walspurger, J. Sommer, Catal. Lett. 93 (2004) 81—84.
[22] S. Tamiyakul, W. Ubolcharoen, D.N. Tungasmita, S. Jongpatiwut, Catal. Today 256 (2015) 325—335.
[23] A.J. Cruz-Cabeza, M.D. Esquivel-Merino, C. Jiménez-Sanchidrián, F.J. Romero-Salguero, Micropor. Mesopor. Mater. 5 (2012) 121—134.
[24] R.A. García, D.P. Serrano, G. Vicente, D. Otero, M. Linares, Stud. Surf. Sci. Catal. 174 (2008) 1091—1094.
[25] Z. Ramli, D. Prasetyoko, S. Endud, Jurnal Teknologi 36 (2002) 41—54.
[26] U. Freese, F. Heinrich, F. Roessner, Catal. Today 49 (1999) 237—244.
[27] A. Corma, M.J. Climent, H. Garcia, J. Primo, Appl. Catal. 49 (1989) 109—123.
[28] W.M. Meier, D.H. Olson, C. Baerlocher, Atlas of Zeolite Structure Types, 4th ed., Elsevier, 1996.
[29] J. Klisáková, L. Cervený, J. Cejka, Appl. Catal., A 272 (2004) 79—86.
[30] (a) A.E.W. Beers, T.A. Nijhuis, F. Kapteijn, J.A. Moulijn, Micropor. Mesopor. Mater. 48 (2001) 279—284;
(b) G. Sartori, R. Maggi, Advances in Friedel-Crafts Acylation Reactions: Catalytic and Green Processes, CRC Press, Boca Raton, FL, USA, 2009.
[31] S.M.T. Almutairi, B. Mezari, G.A. Filonenko, P.C.M.M. Magusin, M.S. Rigutto, E.A. Pidko, E.J.M. Hensen, ChemCatChem 5 (2013) 452—466.
[32] J. Huang, Y. Jiang, V.R.R. Marthala, B. Thomas, E. Romanova, M. Hunger, J. Phys. Chem. C 112 (2008) 3811—3818.
[33] A.J. Maia, B.G. Oliveira, P.M. Esteves, B. Louis, Y.L. Lam, M.M. Pereira, Appl. Catal., A 403 (2011) 58—64.
[34] J. Mérida-Robles, E. Rodríguez-Castellón, A. Jiménez-López, J. Mol. Catal. A 145 (1999) 169—181.
[35] Y.J. Huang, J.A. Schwarz, Appl. Catal. 36 (1988) 163.
[36] A.P. Grosvenor, M.C. Biesinger, R.S.C. Smart, N.S. Mc Intyre, Surf. Sci. 600 (2006) 1771—1779.
[37] M. Mauvezin, G. Delahay, B. Coq, S. Kieger, J.-C. Jumas, J. Olivier-Fourcade, J. Phys. Chem. B 105 (2001) 928—935.
[38] J. Gurgul, K. Latka, I. Hnat, J. Rynkowski, S. Dzwigaj, Micropor. Mesopor. Mater. 168 (2013) 1—6.
[39] K. Gaare, D. Akporiaye, J. Mol. Catal. A 109 (1996) 177—187.
[40] J.N. Armor, Micropor. Mesopor. Mater. 22 (1998) 451—456.
[41] H.P. Decolatti, B.O. Dalla Costa, C.A. Querini, Micropor. Mesopor. Mater. 20 (2015) 180—189.
[42] (a) G.A. Olah, A. Molnar, Hydrocarbon Chemistry, Wiley Interscience, New York, 2003;
(b) D.D. Eley, H. Pines, P.B. Weisz, Advances in Catalysis, vol. 30, Academic Press, New York, 1981.
[43] M. Kantam, K. Ranganath, M. Sateesh, K. Kumar, B. Choudary, J. Mol. Catal. A 225 (2005) 15—20.